

GelMA microneedle-loaded bio-derived nanovaccine shows therapeutic potential for gliomas

Deguang Qin^{a*}, Wenyong Huang^{a*}, Dengke Shen^a, Longyi Chong^a, Zeyu Yang^b, Boyang Wei^b, Xifeng Li^b, Ran Li^b and Wenchao Liu^b

^aDepartment of Neurosurgery, Huangpu People's Hospital of Zhongshan, Zhongshan, China;

^bNeurosurgery Center, Department of Cerebrovascular Surgery, The National Key Clinical Specialty, The Engineering Technology Research Center of Education Ministry of China on Diagnosis and Treatment of Cerebrovascular Disease, Guangdong Provincial Key Laboratory on Brain Function Repair and Regeneration, The Neurosurgery Institute of Guangdong Province, Zhujiang Hospital, Southern Medical University, Guangzhou, China

ABSTRACT

Glioma is the most common primary malignant tumor of the central nervous system in adults. Although immunotherapy, especially tumor vaccines, has made some progress in the treatment of gliomas compared with surgery and radiotherapy. However, the lack of specific or relevant tumor antigens severely limits the further development of tumor vaccines. Here, we report a bio-derived vaccine (TMV@CpG) derived from glioma cell membrane vesicles and carrying TLR9 agonist CpG as adjuvant, which was loaded onto the GelMA microneedle to obtain the microneedle vaccine (MN-TMV@CpG). Microneedle vaccine fully utilize the innate immune cells rich in the skin, inducing stronger cellular immune responses. In subcutaneous tumor models, MN-TMV@CpG reversed the immune-suppressing microenvironment of tumor, and effectively inhibited tumor progression. In an intracranial tumor model, MN-TMV@CpG significantly prolonged the survival duration and induced stronger immune memory responses in tumor bearing mice when combined with anti-PD1 mAb. These results suggest that bio-derived nanovaccines can be used as a potential antitumor immunotherapy strategy.

ARTICLE HISTORY

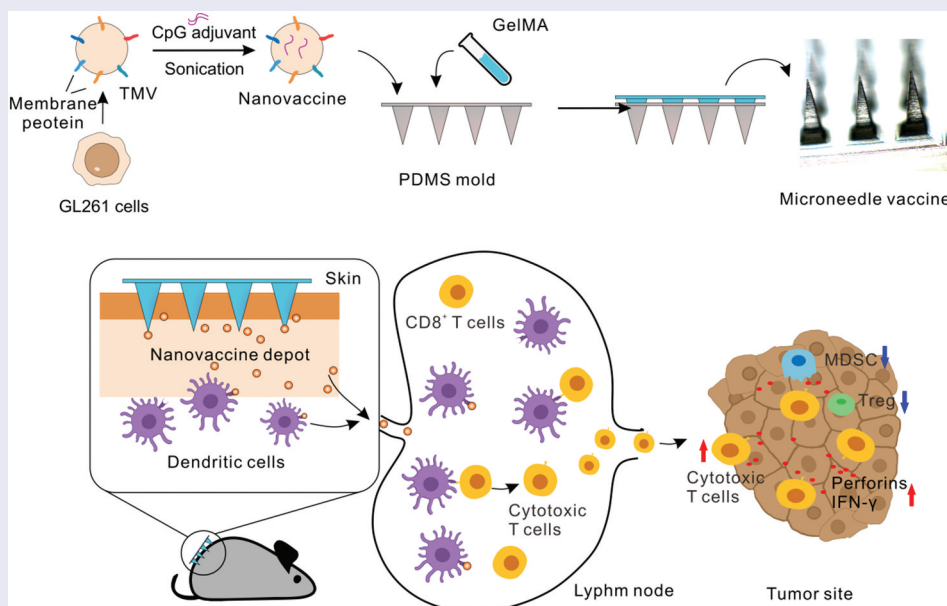
Received 2 September 2024

Revised 28 October 2024

Accepted 1 November 2024




KEYWORDS

Bio-derived nanovaccine; GelMA gel; microneedle vaccine; glioma; cellular immunity



IMPACT STATEMENT

We developed a microneedle vaccine with a multivalent antigen and adjuvant CpG that induces strong anti-tumor immunity and immune memory, thereby prolonging survival of glioma-bearing mice.

CONTACT Ran Li  mayo_2012@126.com; Wenchao Liu  liuwenchao@smu.edu.cn  Neurosurgery Center, Department of Cerebrovascular Surgery, The National Key Clinical Specialty, The Engineering Technology Research Center of Education Ministry of China on Diagnosis and Treatment of Cerebrovascular Disease, Guangdong Provincial Key Laboratory on Brain Function Repair and Regeneration, The Neurosurgery Institute of Guangdong Province, Zhujiang Hospital, Southern Medical University, No. 253, Industrial Avenue Zhong, Haizhu District, Guangzhou, Guangdong, China

*These authors contributed to the work equally and should be regarded as co-first authors.

© 2024 The Author(s). Published by National Institute for Materials Science in partnership with Taylor & Francis Group.

This is an Open Access article distributed under the terms of the Creative Commons Attribution-NonCommercial License (<http://creativecommons.org/licenses/by-nc/4.0/>), which permits unrestricted non-commercial use, distribution, and reproduction in any medium, provided the original work is properly cited. The terms on which this article has been published allow the posting of the Accepted Manuscript in a repository by the author(s) or with their consent.

1. Introduction

Gliomas are the most common primary malignant tumors of the central nervous system and exist within the intrinsic blood-brain barrier with a highly heterogeneous, aggressive, and specific tumor microenvironment [1,2]. This poses a great challenge for the treatment of gliomas. Currently, gliomas are treated with surgical resection, radiotherapy and chemotherapy. However, gliomas have a poor prognosis due to their characteristics that make them difficult to completely resect in treatment, high recurrence and mortality rate [3–5]. In recent years, the effectiveness of immunotherapy has been demonstrated in a wide range of tumors. Researchers have used chimeric antigen receptor (CAR) T cell therapy [6–8], lyssavirus therapy [9–11], immune checkpoint therapy [12–14] and tumor vaccines [15–18] to try to treat glioma. For the development of glioma tumor vaccines, the vaccine CDX-10, which targets a single tumor antigen, did not show a significant improvement in survival in the treatment versus control group in a phase III clinical trial [19]. The results of a phase III clinical trial using a dendritic cell (DC) vaccine loaded with autologous glioma cell lysates showed a significant prolongation of patient survival, with a median survival of 23.1 months postoperatively in the treatment group and 2- and 3-year survival of 46.2% and 25.4%, respectively [20]. Therefore, the development of vaccines for glioblastoma can be carried out in two ways, one is how to activate a strong innate immune response by virtue of a limited number of antigens and reduce the activity of immunosuppressive cells, thus facilitating the function of DCs in antigen processing and presentation. On the other hand, increasing the antigen variety amplifies the recognition of tumor cells by DCs and T cells, resulting in a stronger antitumor response.

Currently, tumor therapy is enhanced by increasing DCs targeting and using biomimetic vehicles [21,22]. In particular, tumor cell membrane (TMV) inherits all specific and relevant antigenic proteins of tumor cells [23]. Compared with whole-cell lysates, TMV does not contain the genetic material of tumor cells and has a good safety [24,25]. Tumor vaccines developed based on TMV have been applied in the treatment of various tumors such as melanoma [26], breast cancer [27], and non-small cell lung cancer [28]. Hence, it is reported here a bio-derived nanovaccine based on TMV of glioma as a carrier and antigen source for nanovaccines. Meanwhile, the fortification of vaccine-induced antitumor response (TMV@CpG) by introducing the TLR9 agonist CpG into TMV. In addition, studies have shown that transdermal administration induces stronger humoral and cellular immune responses compared to subcutaneous administration [29–31]. Microneedles, as a classical transdermal drug delivery

method, not only deliver drugs intradermally in a noninvasive manner, but also the high patient compliance and convenience make them a highly promising vaccination modality [32–34]. We used GelMA hydrogel to fabricate microneedles and loaded nanovaccines onto the microneedles to prepare a microneedle vaccine (MN-TMV@CpG, Scheme 1). The passive diffusion of particles within the skin and the active uptake of intradermal-resident DCs were utilized to induce a strong anti-tumor immune response. Furthermore, the combination of anti-PD1 mAb and vaccine for intracranial glioma not only significantly prolonged the survival of mice, but also induced a strong immune memory. Thus, microneedle-loaded bio-derived nanovaccines are expected to be an effective means of treating gliomas.

2. Materials and methods

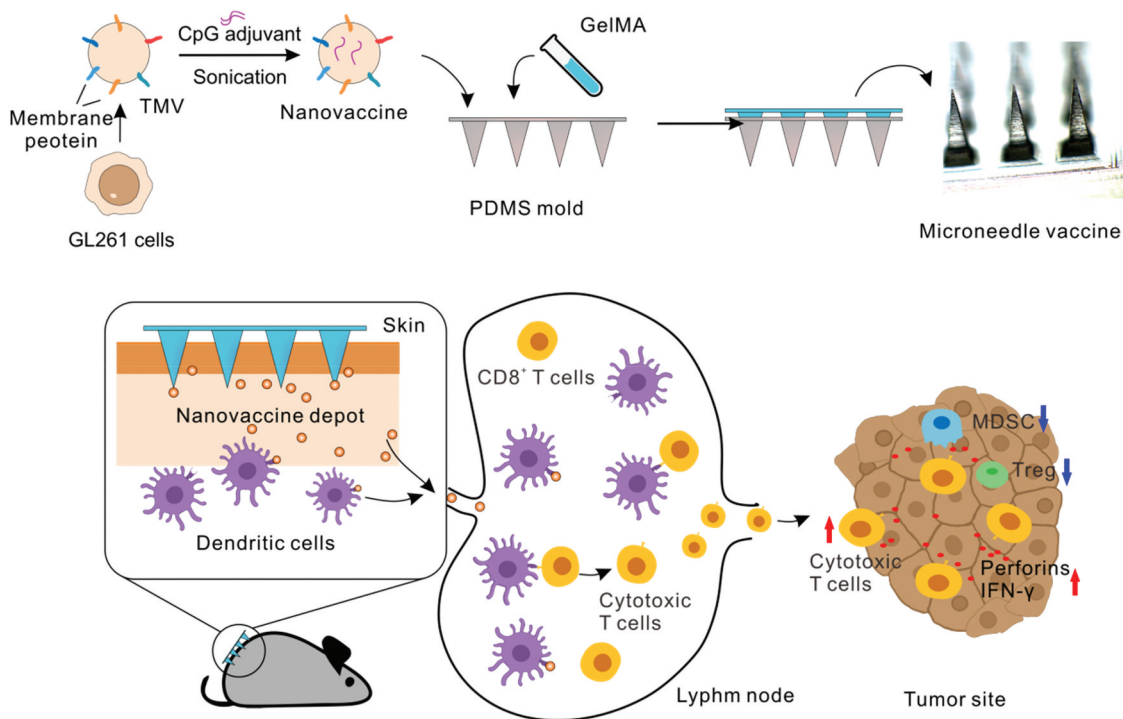
2.1. Materials

Gelatin methacryloyl (GelMA) and Lithium phenyl (2,4,6-trimethylbenzoyl) phosphinate (LAP) were purchased from EFL-Tech Co.,Ltd, China. Fluorescent dye Cy5, DAPI and Lyso-TrackerGreen were purchased from Beyotime, China. Anti-mouse PD1 was purchased from Bioxcell, U.S.A. CpG ODN was purchased from Sangon, China. DMEM, RPMI 1640, Fetal Bovine Serum, Trypsin and phosphate buffered solution (PBS) were purchased from Gibco, U.S.A. BCA protein assay kit, RIPA lysis buffer, Protease inhibitor, Permeabilization Wash Buffer, Fixative buffer were purchased from ThermoFisher, U.S.A. MTT, IL-4, Granulocyte-macrophage colony stimulating factor (GM-CSF) and Mouse bone marrow lymphocyte kit were purchased from Solarbio. The mouse IL-12 Elisa Kit, mouse IL-6 Elisa Kit and mouse TNF- α Elisa Kit were purchased from Biolegend (U.S.A.).

The following anti-mouse mAb were purchased from Biolegend, U.S.A.: Zombie Aqua™ Fixable Viability Kit, CD16/32 antibody, CD45-APC/Fire750, CD11c-PE, CD86-FITC, CD3-PerCP/Cy5.5, CD4-FITC, CD8-AF700, CD69-BV421, CD44-PE, CD62L-APC, CD11b-FITC, Gr-1-AF647, Ki67-PE/Cy7, IFN- γ -APC.

2.2. Cell and mice

DC2.4 and GL261 cell lines were purchased from the American Type Culture Collection (ATCC). DC2.4 was cultured in RPMI1640 medium. GL261 was cultured in DMEM medium. All cell lines were cultured in a 37°C and 5% CO₂ humidified incubator. The bone marrow cells were isolated from the mouse tibia and femur by mouse bone marrow lymphocyte kit and resuspended in RPMI1640 medium containing 20 ng/mL GM-CSF



Scheme 1. Schematic illustration of microneedle vaccine and their eliciting antitumor immune responses. Preparation process of tumor membrane vesicle nanovaccine (Tmv) and loading into microneedle patch. Microneedle vaccines form depot at the injection site, where a portion of the nanovaccine is taken up by skin-resident DCs leading to DC activation, and the other portion carries on draining lymph nodes to activate DCs through size effect, thus inducing a stronger anti-tumor immune response.

and 10 ng/mL IL-4. The medium was semi-changed every 3 days, and the suspension cells and semi-adherent cells were collected on the 6th day to obtain Bone marrow-derived dendritic cells (BMDCs).

Animal studies were conducted with the approval of the Experimental Animal Management and Use Committee and Experimental Animal Ethics Committee of Southern Medical University. C57BL/6J mouse (female, 6–8 weeks) were housed in specific pathogen-free conditions and randomly grouped according to the experimental plan.

2.3. Preparation of nanovaccines

GL261 cells were collected and resuspended in 1% Protease inhibitor PBS buffer. The cells were crushed by Ultrasonic crusher (Scientz, China) in ice bath. Subsequently, the membrane vesicles were obtained by gradient centrifugation. The pellet was resuspended with PBS to obtain TMV through a 0.8 μm filter membrane, and then hydrated with PBS buffer containing 200 μg/mL CpG with ice bath conditions to obtain the nanovaccine (TMV@CpG). The protein and cpg contents of nanovaccine were quantified by BCA kit and Nanodrop, respectively.

2.4. Characterization of nanovaccines

GL261 cells, TMV and TMV@cpg were lysed with Ripa lysis buffer, the loading buffer was added and

the protein was denatured by incubation in a 95°C water bath for 10 min. The equal amount of the sample was then loaded onto the 10% SDS-PAGE gel. After running the gel, stain it with Coomassie blue buffer and microwave for 1 minute. The dye gel was decolorized at high temperature in ddH₂O and imaged with gel imaging system (Tanon, China).

The TMV@CpG was placed on the copper mesh and stained with uranium acetate. After the copper mesh was dried, the morphology of the nanovaccine was observed by TEM (JEOL, Japan).

The particle diameter distribution and surface zeta potential of nanovaccine were tested using Zetasize Nano ZS (Malvern, United Kingdom).

The nanovaccine was placed in a constant temperature shaking bed at 37°C at 100 rpm. Samples were collected at different time points to test the in vitro release behavior of CpG using Nanodrop.

2.5. Physiological functions of nanovaccines

The cytotoxicity of nanovaccine was evaluated by MTT assay. DC2.4 cells were plated in 96 well plates at a volume of 200 μL and a density of 5 × 10⁴/mL for 24 hours. The cells were treated with different concentrations of TMV, 6 parallel wells at each concentration, and incubated for 24 hours. The medium was removed and 100 μl PBS and 10 μL MTT were added to each well. After 4 hours, the supernatant was removed and 100 μl DMSO was added to each well.

The plates were placed in a horizontal shaker and shaken for 10 minutes. The absorbance of the plates at 570 nm was measured by enzyme-labeled instrument (Biotek, United States).

The absorption of nanovaccine by BMDC and the ability of lysosome escape were observed by Confocal laser scanning microscope (CLSM, ZEISS, German). BMDCs were placed in confocal petri dishes and incubated for 24 hours. Medium was removed, and fresh RPMI1640 medium (protein, 10 $\mu\text{g}/\text{mL}$) containing Cy5- labeled nanovaccine was added and incubated for 4 hours. The medium was removed and the lysosomes and nuclei were labeled with FITC and DAPI, respectively. The ability of particles to be absorbed by BMDC and lysosome escape was observed by CLSM.

At the same time, BMDCs were plated in 24-well plates and incubated for 4 hours. 100 μL Cy5 fluorescent dye (1 $\mu\text{g}/\text{mL}$) was mixed with 100 μL TMV (protein, 100 $\mu\text{g}/\text{mL}$) and magnetically stirred at 4°C for 24 hours, and then dialyzed using a 1000 D dialysis membrane in 1 L of PBS buffer for 12 hours. The PBS buffer was replaced and the Cy5-labeled nanovaccine was obtained after 12 hours of dialysis. The Cy5-labeled nanovaccines (protein, 10 $\mu\text{g}/\text{mL}$; CpG, 10 $\mu\text{g}/\text{mL}$) were added to stimulate immature BMDCs. Cells and cell culture medium were collected. Cells were stained with fixable live/dead differentiating dye Zombie Aqua™ Fixable Viability Kit. Subsequently, non-specific binding was blocked using CD16/32 to incubate with cells for 15 min. BMDCs were stained with CD11c and CD86. Finally, the unbound dyes were removed, and the data were analyzed by flow cytometry (Attune Nxt, United States), and quantitative analysis by FlowJo. Meanwhile, based on the literature, we further analyzed the effect of CpG on the activation of BMDCs [35]. The secretion of pro-inflammatory factors by BMDCs treated with different samples was examined using Elisa kit instructions for IL6, IL12 and TNF- α .

2.6. Preparation and characterization of microneedle vaccine

Microneedle vaccine preparation was performed using the polydimethylsiloxane microneedle mold of a 10×10 array with a needle body height of 800 μm and a bottom width of 200 μm . The ambient temperature was always controlled at 4°C during the preparation process. First, the 15% (w/v) GelMA solution containing 0.25% (w/v) LAP and TMV (or tmv@cpg) was deposited on the tip area of the mold and the mold was placed in a vacuum chamber to remove the bubbles. Next, the mold was filled with the 15% (w/v) GelMA solution containing 0.25% (w/v) LAP and the excess solution was removed. The mixture was gelatinized by 405 nm UV irradiation for 30 seconds. The microneedle vaccine was obtained by mold release

after low temperature drying. Microneedles were stripped from the substrate and placed in 2 mL of pH = 7.4 PBS buffer, heated to promote solubilization, and the microneedle-loaded proteins were quantified using a BCA kit after complete solubilization.

The microneedles were stripped from the substrate and placed in 2 mL of pH = 7.4 PBS buffer, and the liquid was placed in the 37°C shaker (180 rpm). The release behavior of the particles was monitored by taking 100 μL of the liquid at different time points and assaying the protein content of the liquid using a BCA kit.

The morphology of the microneedle vaccine was obtained by digital stereomicroscopy (SMZT4, Chongqing Aote Optics).

The microneedle vaccine loaded with Cy5-labeled TMV@CpG was inoculated into fresh pig skin. After 1 hour, remove the microneedles and use CLSM to observe the penetration of the nanoparticles into the skin.

2.7. Effect of microneedle vaccine on immune microenvironment in draining lymph nodes

Preparation of microneedle vaccines using Cy5-labeled nanovaccine. The microneedle vaccine was inoculated into the dorsal skin of mice. Mice were sacrificed at different time points. The inguinal lymph nodes of mice were taken and fluorescence imaging was performed using a small animal in vivo imaging instrument to study the aggregation behavior of particles in the inguinal lymph nodes.

On the other hand, the mice were vaccinated with microneedles on their backs. After 24 hours, the mice were sacrificed, and the inguinal lymph nodes were taken to prepare single cell suspensions. The single cell suspension was treated with fixable live/dead differentiating dye and CD16/32 antibody. Subsequently, the single cell suspension was stained with the following antibodies: CD45, CD11c, CD86, CD3, CD4 and CD8. Finally, the unbound dyes were removed, and the data were analyzed and quantified.

2.8. In vivo tumor models

Subcutaneous tumor model. 4×10^5 GL261 cells were injected subcutaneously into mice to observe their growth. Tumor size was calculated as follows: tumor size = width*width*length *0.5. Vaccination began on Day 10. Three doses of the vaccine (containing tumor cell membrane protein 10 μg , CpG 10 μg) were administered every 7 days. Body weight and tumor size were measured every 3 days. On Day 31, mice were killed, tumors removed and made into single cell suspensions for flow cytometry stained and analyzed.

Intracranial tumor model. 2×10^5 GL261 cells were implanted into the mouse brain using a stereotactic

fixation device. On Day 5, tumor formation was determined using luciferase substrate bioluminescence imaging and treatment began. Anti-PD1 antibody was injected into the tail vein every 3 days (200 µg/dose) for five times. Three doses of microneedle vaccine are given every 7 days. The survival rate of mice was detected continuously. On Day 26, the mice were sacrificed and the tumor was prepared with single cell suspension for flow cytometry. The heart, liver, spleen, lung and kidney were obtained for H&E staining.

2.9. Analysis of immune microenvironment

For the spleen, the first use of red blood cell lysate to remove red blood cells, single cell suspension obtained by screening mesh. The single cell suspension was prepared by direct grinding and screening. Then, the suspension was treated with fixable live/dead differentiating dye Zombie Aqua™ Fixable Viability Kit and CD16/32. Subsequently, the cells were stained with the following antibodies: CD45, CD3, CD4, CD8, CD69, CD44, CD62L, CD11b and Gr-1. For further intracellular staining, the cells were fixed and permeabilized using fixative buffer and Permeabilization Wash Buffer, and then stained with IFN-γ and Ki67. Finally,

the unbound dyes were removed, and the data were analyzed and quantified.

2.10. Statistics

The statistical significance of difference between experimental groups was analyzed with One way or two-way ANOVA determined by Tukey post-hoc tests using GraphPad Prism 9. * $p < 0.05$, ** $p < 0.01$ or *** $p < 0.001$. All the values were reported as mean ± SEM.

3. Results and discussion

3.1. Fabrication and characterization of bio-derived nanovaccine

The preparation of the bio-derived nanovaccine was divided into two main steps: (I) TMV of tumor cells was obtained by gradient centrifugation and membrane extrusion, and (II) the CpG ODN was loaded into TMV by sonication (Figure 1(a)). The obtained TMV@CpG nanovaccine utilized the cell membrane protein of GL261 as antigen and the TLR9 agonist CpG as adjuvant. To verify the successful preparation of the vaccine, the changes in membrane proteins

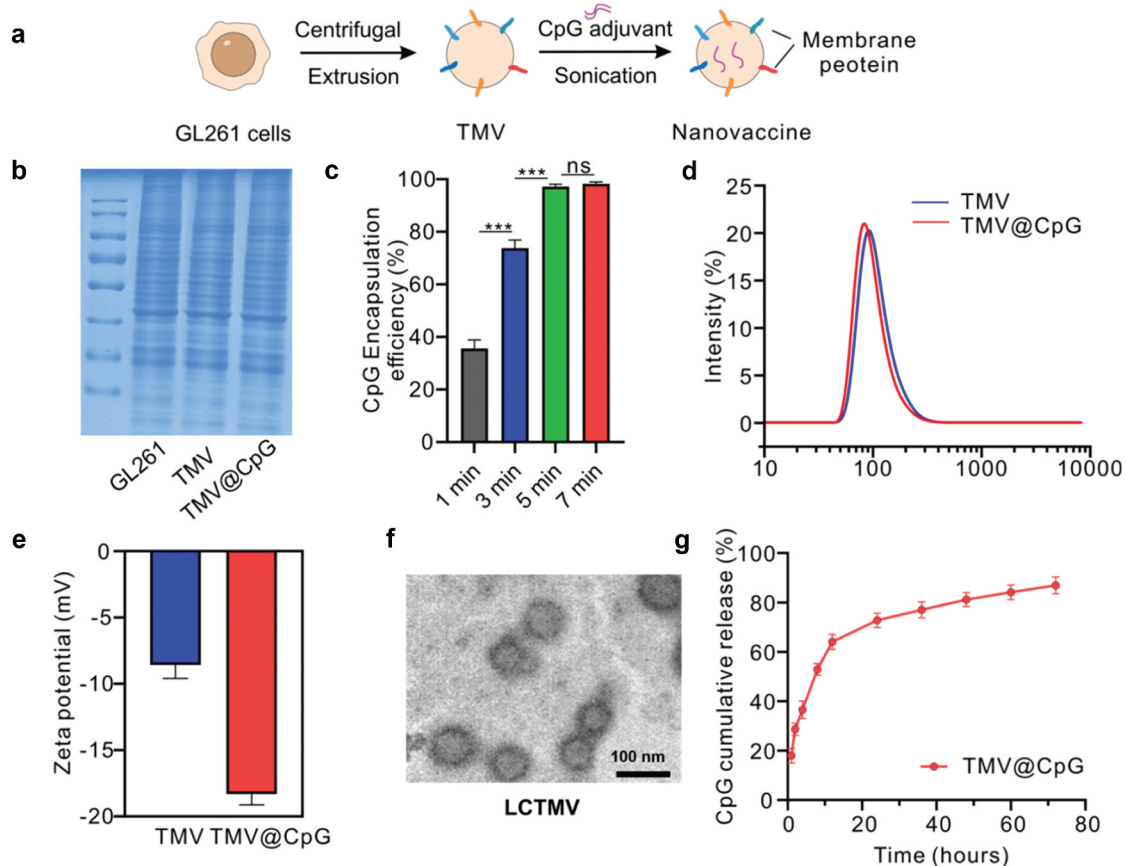


Figure 1. Fabrications and characterization of nanovaccine. (a) Schematic of TMV nanovaccine loaded with CpG adjuvant (TMV@CpG). (b) SDS-page image of GL261, TMV and TMV@CpG. (c) The encapsulation efficiency of CpG prepared by a sonication duration of 1, 3, 5 and 7 minutes ($n = 5$). The particle size distribution (d) and Zeta potential analyses (e) of TMV and TMV@CpG prepared by a sonication duration of 5 minutes ($n = 3$). (f) TEM image of TMV@CpG. (g) CpG release behavior of TMV@CpG in PBS buffer solution ($n = 3$).

before and after preparation were analyzed by Coomassie blue staining, which showed that the preparation process did not result in the loss of membrane proteins and that the nanovaccine inherited all the proteins of TMV (Figure 1(b)). Subsequently, the fabrication method of the vaccine particles was optimized by detecting the encapsulation rate of CpG in the particles with different sonication durations (Figure 1(c)). The results showed that the encapsulation rate of CpG in TMV was only 35.6% when the sonication duration was 1 min. With the increase of sonication duration, the encapsulation rate gradually increased. When the ultrasound duration was 5 min, the encapsulation rate reached 97.2%, and compared with the preparation method of longer duration, the encapsulation rate of CpG by the particles did not increase significantly. Therefore, we choose the sonication duration of 5 min to prepare the subsequent TMV@CpG nanovaccines. The particle size distributions of TMV and TMV@CpG are shown in Figure 1(d), with average particle sizes of 106 nm and 101 nm, respectively, both of which were narrower, and the addition of CpG did not cause a significant change in particle size. In contrast to the particle size, the addition of electronegative CpG caused a decrease in the surface zeta potential of TMV@CpG, which was -18.3 mV (Figure 1(e)). TEM images showed that TMV@CpG was a globular particle with a double-layer membrane structure (Figure 1(f)). The results of CpG release behavior in vitro showed that CpG in TMV@CpG was able to release 52.8% within 8 hours and slowly over the subsequent time, reaching a CpG release rate of more than 80% at 48 hours (Figure 1(g)). Together, these results suggested the successful preparation of a bio-derived nanovaccine that could provide the basis for effective immune system activation due to its tumor-specific and relevant antigenic proteins and size effect.

3.2. Bio-derived nanovaccine promoted internalization and activation of DCs

It was investigated the effect of activation of innate immunity by bio-derived nanovaccines in vitro. The results of MTT experiments exhibited good biosafety of the TMV material, with the survival rate of DC2.4 cells still exceeding 80% at a concentration of 180 $\mu\text{g}/\text{mL}$, and less than 60% at a concentration of up to 320 $\mu\text{g}/\text{mL}$ (Figure 2(a)). Subsequently, the uptake of nanoparticles by innate immune cells BMDCs was investigated. Compared with the PBS group (0.2%), the percentage of BMDCs treated with TMV (58.3%) or TMV@CpG (67.1%) that ingested particles was significantly higher (Figure 2(b)). We further used CLSM to observe the uptake of vaccine particles by BMDCs and the lysosomal escape of particles. Like the flow cytometry results, the nanovaccines could be

uptaken by BMDCs, where TMV@CpG was able to achieve a higher degree of lysosomal escape level intracellularly, which induced a stronger immune response (Figure 2(c)). Meanwhile, we investigated the expression level of CD86, an activation marker for BMDCs, induced by the nanoparticles. Compared with the PBS group (13.2%), the TMV and TMV@CpG groups induced stronger CD86 expression levels of 34.2% and 49.3%, respectively (Figure 2(d)). In addition, the nanovaccines induced BMDCs to secrete more TNF- α , IL-6, and IL-12 pro-inflammatory factors (Figure 2(e)). The introduction of CpG led to a significant enhancement in the level of pro-inflammatory factors secreted by TMV@CpG-treated BMDCs, favoring the activation of downstream helper T cells, CD8⁺ T cells and NK cells to generate a cellular immune response. The above results indicated that the bio-derived nanovaccine could significantly enhance the uptake of particles by BMDCs as well as induce stronger activation levels of BMDCs, which facilitates antigen presentation and has the potential to induce a stronger cellular immune response.

3.3. Activation of DCs and T cells by TMV@CpG in microneedle patch

Following the determination that the biogenic nanovaccine was able to awaken a stronger innate immune response in the body, we loaded the nanoparticles onto GelMA microneedles. The microneedle vaccine was prepared by mixing the nanovaccine with GelMA, forming a hydrogel using a UV light source with the participation of a LAP cross-linking agent, and obtaining the microneedle vaccine by low temperature drying and stripping (Figure 3(a)). The three-dimensional network structure of the GelMA gel promotes the slow release of vaccine particles and the formation of antigen depot at the vaccination site, resulting in a sustained stimulatory effect on the organism. The BCA results showed that the membrane protein content of the four batches of microneedle vaccines did not show significant fluctuation, and the protein content was about 10 μg in both MN-TMV and MN-TMV@CpG (Figure 3(b)). Meanwhile, the results showed that the microneedles released vaccine particles rapidly within 1 h and more than 90% of the vaccine particles were released at 4 h (Figure 3(c)). Then, we studied the penetration of microneedles into the skin. Microneedle vaccines with Cy5-labeled nanoparticles were administered to the skin, and the residence of the particles in the skin was observed. The results displayed that the microneedles had sufficient mechanical strength to penetrate the skin and could deliver the particles to an intradermal depth of more than 140 μm (Figure 3(d)). This demonstrated that the microneedle vaccine was able to deliver the particles into the skin

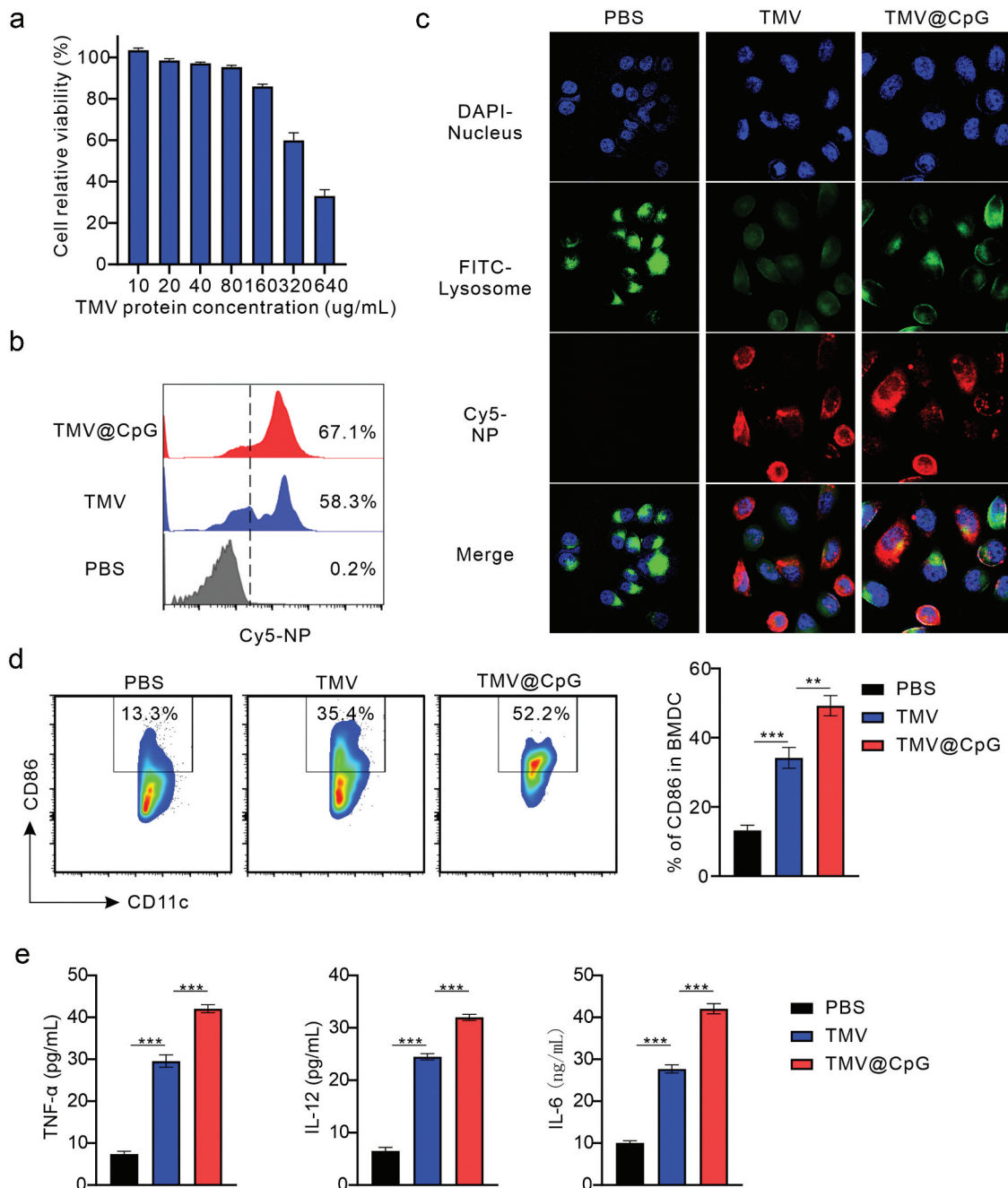


Figure 2. Bio-derived nanovaccines enhance the uptake of antigens by BMDCs and promote the maturation of BMDCs. (a) Evaluation of the toxicity levels of TMV to DC2.4 ($n = 6$). (b) Cellular uptake histograms of Cy5-labeled nanovaccine measured by flow cytometry ($n = 3$). (c) Representative CLSM images showed BMDCs incubated with TMV and TMV@CpG for 4 h, respectively. (d) Representative dot plots and quantitative analysis of the activation marker CD86 of BMDCs after incubated with TMV and TMV@CpG for 24 h ($n = 5$). (e) Secretion of cytokine $\text{tnf-}\alpha$, IL-6 and IL-12 in the supernatant of cultured BMDCs measured by Elisa ($n = 5$).

and fully utilize the skin-resident DCs, macrophages and other innate immune cells to complete the delivery of antigens, thereby inducing a stronger immune response. Further, the stability of microneedle vaccine preparation was investigated by detecting the membrane protein content of microneedle prepared in different batches after reconstitution.

The enrichment of particles in lymph nodes was further explored and the results showed that MN-TMV and MN-TMV@CpG were able to enrich the lymph nodes within 4 hours of vaccination, and the

highest level of particle enrichment was observed at 24 hours, followed by gradual attenuation (Figure 3(e)). This provides a solid basis for vaccine particles to induce DC activation in draining lymph nodes to promote cellular immune responses. The in vivo data showed that $\text{CD11c}^+\text{CD86}^+$ was significantly elevated in the draining lymph nodes of the MN-TMV group (39.4%) and the MN-TMV@CpG group (53.8%), using the blank microneedle group (MN, 18.4%) as a control (Figure 3(f)). Meanwhile, it was detected the changes of T cells infiltration in the draining lymph nodes.

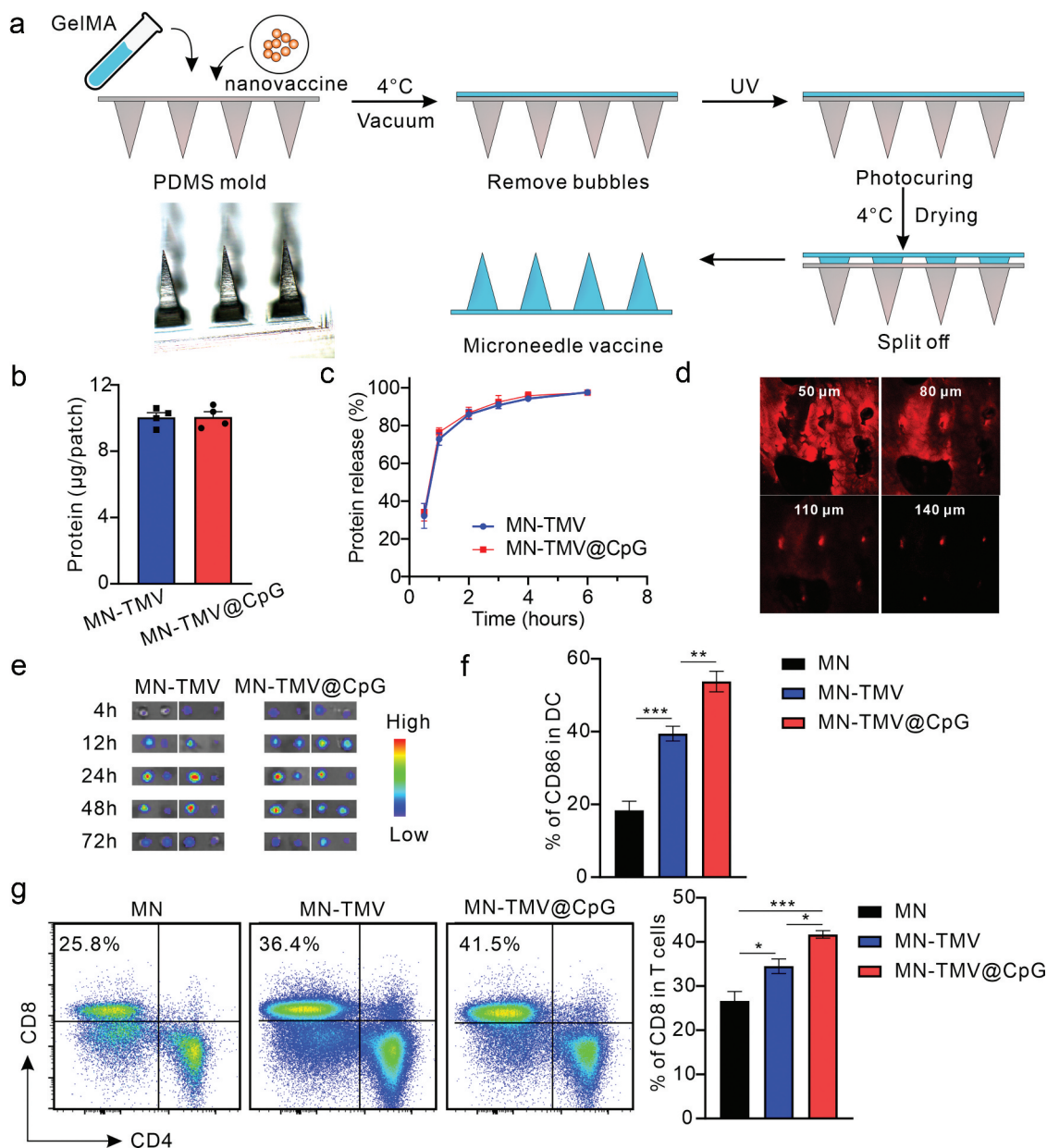


Figure 3. Microneedle vaccine induced strong antigen-presenting cells response and CD8⁺ T cells aggregation in drainage lymph nodes. (a) Microneedle vaccine preparation method. GelMa was used as the material for the needle body, and a three-dimensional mesh structure encapsulating the nano-vaccine particles was formed by cross-linking through UV irradiation, so that the vaccine could produce a continuous stimulation of the body's immune system, thus inducing a stronger antigen-specific immune response. (b) The stability of loading capacity of tumor cell membrane protein in microneedle ($n = 3$). (c) In vitro release profiles of nanoparticles from microneedle vaccines ($n = 3$). (d) CLSM images of the depth of microneedle loaded Cy5-TMV@CpG penetration of the skin. (e) Enrichment of vaccine particles in inguinal lymph nodes at different times after vaccination ($n = 2$). (f) Quantitative analysis of CD86 on DCs in the drainage lymph nodes 24 hours after vaccination, analyzed by flow cytometry ($n = 5$). (g) Representative dot plots and quantitative analysis of CD8⁺ T cells in the drainage lymph nodes 24 hours after vaccination, analyzed by flow cytometry ($n = 5$).

The proportions of CD8⁺ T cells were 26.7%, 34.5%, and 41.7% in the MN, MN-TMV, and MN-TMV@CpG groups, respectively (Figure 3(g)). Together, these results demonstrated that microneedle vaccines, especially MN-TMV@CpG, could promote the uptake of antigen by DCs in the draining lymph nodes and significantly enhance the activation level of DCs. Concomitantly, activated DCs elicited a higher proportion of T-cell infiltration in the draining lymph nodes, leading to a stronger cellular immune response.

3.4. MNTMV@CpG reverse immunosuppression of the tumor microenvironment to inhibit tumor progression

First, the glioma model was established subcutaneously in mice using GL261 to study the anti-tumor effect of the microneedle vaccine (Figure 4(a)). The results showed that at Day 31, the average tumor sizes of mice in the MN, MN-TMV, and MN-TMV@CpG groups were 1487.6 mm³, 963.7 mm³ and 479.4 mm³,

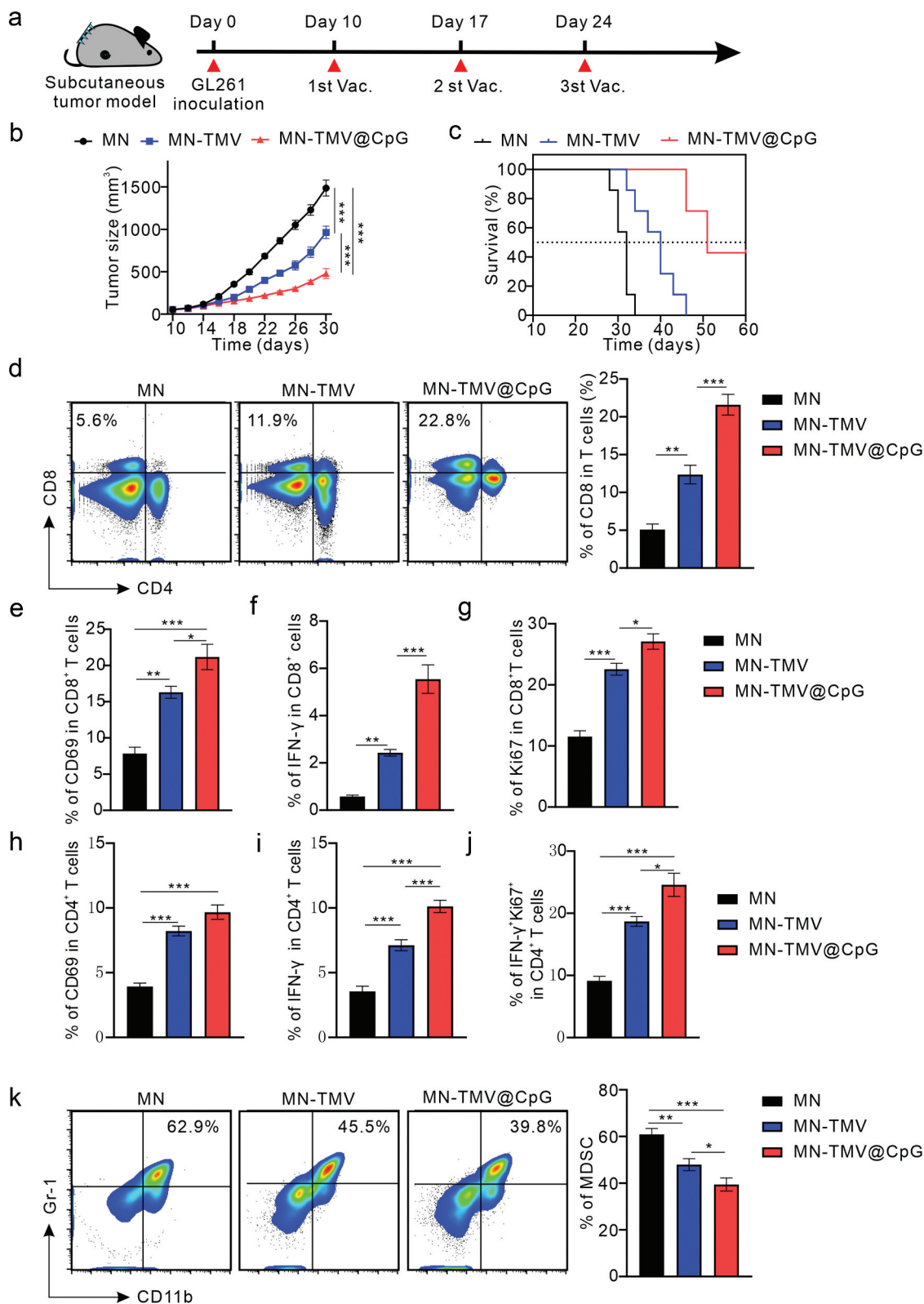


Figure 4. Microneedle vaccine improved the anti-tumor effect in subcutaneous tumor model. (a) The protocol of vaccination with MN, MN-TMV and MN-TMV@CpG in C57BL/6J mice with GL261 tumor model. On day 10, the first dose of vaccine was administered, followed by vaccination on day 17 and 24. Flow cytometry analysis of tumors was performed on day 31. Tumor volume monitoring ended on day 31. (b) Tumor growth kinetics in different treatment groups ($n = 7$). (c) Survival curves in different treatment groups ($n = 7$). (d) Representative dot plots and quantitative analysis of CD8⁺ T cells in tumor excised from mice in different treatment groups, analyzed by flow cytometry ($n = 5$). Quantification of CD8⁺CD69⁺ T cells (e), CD8⁺IFN- γ ⁺ T cells (f) and CD8⁺ Ki67⁺ T cells (g) in the TME ($n = 5$). Quantification of CD4⁺CD69⁺ T cells (h), CD4⁺IFN- γ ⁺ T cells (i) and CD4⁺IFN- γ ⁺Ki67⁺ T cells (j) in the TME ($n = 5$). (k) Representative dot plots and quantitative analysis of MDSCs in the TME, analyzed by flow cytometry ($n = 5$).

respectively (Figure 4(b)). This indicated that the microneedle vaccine was able to significantly inhibit tumor growth, with the most pronounced slowing of the degree of tumor growth in the MN-TMV@CpG group. On the other hand, the survival of mice vaccinated with microneedle vaccine was significantly prolonged (Figure 4(c)). Compared with the MN group (32 days), the median survival of mice in the MN-TMV group and the MN-TMV@CpG group were 40 days and 51 days, respectively. The median survival of mice in the MN-TMV@CpG group was 1.25 and 1.59 times that of the MN and MN-TMV groups, respectively. These results indicated that the microneedle vaccine MN-TMV@CpG was able to significantly alleviate tumor progression and prolong the survival of tumor-bearing mice.

To investigate the antitumor mechanism, it was analyzed the changes in the tumor microenvironment using flow cytometry. Figure 4(d) showed that the proportions of CD8⁺ T cells in the tumor microenvironment in MN, MN-TMV, and MN-TMV@CpG groups as 5.1%, 12.4% and 21.6%, respectively. The level of CD8⁺ T cell infiltration in the tumors of the MN-TMV@CpG group was significantly increased. Furthermore, it was analyzed the changes of CD8⁺ T cell subpopulation proportions. The proportion of activated CD8⁺ T cells (CD3⁺CD8⁺CD69⁺) at the tumor site of mice vaccinated with microneedle vaccine was significantly up-regulated were 7.8%, 16.3% and 21.2% for MN, MN-TMV and MN-TMV@CpG groups, respectively (Figure 4(e)). Likewise, we observed that the levels of CD8⁺ T cells secreting the pro-inflammatory cytokine IFN- γ in the MN, MN-TMV and MN-TMV@CpG groups were 0.6%, 2.4% and 5.5%, respectively (Figure 4(f)). This indicated that the microneedle vaccine not only promoted the aggregation of CD8⁺ T cells at the tumor site, but also greatly increased the activation and tumor cell killing levels of the aggregated CD8⁺ T cells, resulting in a better antitumor effect. In addition, the proliferation level of CD8⁺ T cells (CD3⁺CD8⁺Ki67⁺) in the tumors of mice vaccinated with microneedle vaccine was also significantly enhanced (Figure 4(g)). This facilitated the continuous activation of CD8⁺ T cells to kill tumor cells for the purpose of inhibiting tumor growth. It was further analyzed the changes of CD4⁺ T cell subsets. The results showed that the proportions of CD4⁺CD69⁺ T cells, CD4⁺IFN⁺ T cells and CD4⁺IFN⁺Ki67⁺ T cells appeared to be upregulated to different degrees (Figure 4(h-j)). This indicated that CD4⁺ T cells tend to differentiate towards Th1-type cells, thereby inducing a stronger cellular immune response. On the other hand, the changes of myeloid-derived suppressor cells (MDSC) infiltration in the tumor were analyzed. The results showed that the proportion of MDSC was significantly down-

regulated in the MN-TMV group (47.9%) and the MN-TMV@CpG group (39.4%) compared with the MN group (60.9%) (Figure 4(k)). These results indicated that the excellent antitumor effects of microneedle vaccines were mainly achieved via stimulating the activation and proliferation of CD8⁺ T cells in the tumor microenvironment, reducing MDSC infiltration, and thus reversing the immunosuppressed tumor microenvironment.

3.5. MN-TMV@CpG efficiently inhibited progression of intracranial tumors

The presence of a blood-brain barrier and a brain microenvironment composed mainly of microglia, astrocytes, oligodendrocytes, and neurons makes it difficult for peripheral immune cells to infiltrate intracranial gliomas to play a role in inhibiting tumor growth. The results of the mouse glioma subcutaneous model experiments showed that the microneedle vaccine demonstrated a good inhibitory effect, and we further explored the inhibition of intracranial gliomas by the vaccine, while introducing the anti-PD1 monoclonal antibody for the combination treatment. After confirming the successful construction of the intracranial glioma model, mice were randomly divided into four groups, and the treatment protocols are shown in Figure 5(a). The results showed that the median survival of the MN group, MN-TMV group, MN-TMV@CpG group, Anti-PD1 group and MN-TMV@CpG+anti-PD1 group were 24 days, 33 days, 39 days, 30 days and 45 days, respectively (Figure 5(b)). Compared with the MN group, the median survival of mice in the MN-TMV@CpG group vaccinated alone was prolonged by 15 days, and that of mice in the MN-TMV@CpG+Anti-PD1 group in the combined treatment group was prolonged by 21 days. This indicated that the microneedle vaccine could not only inhibit subcutaneous tumor progression, but also inhibit intracranial tumor growth. Meanwhile the addition of anti-PD1 mAb could further eliminate the inhibitory effect of immunosuppressive cells on T cells in the tumor, so the survival of mice in the MN-TMV@CpG+Anti-PD1 group of the combined treatment group was significantly prolonged. The body weight of mice in the MN-TMV@CpG group and the MN-TMV@CpG+Anti-PD1 group did not bleed significantly during treatment (Figure 5(c)).

The infiltration levels of immune memory cells in the spleens of the various groups of tumor-bearing mice were analyzed, and we found that the proportion of central memory T cells (Tcm) was significantly elevated in both the vaccine treatment alone and the combination treatment groups (Figure 5(d,e)). In particular, Tcm of MN-TMV@CpG+Anti-PD1 were significantly upregulated in the combination treatment group compared to the

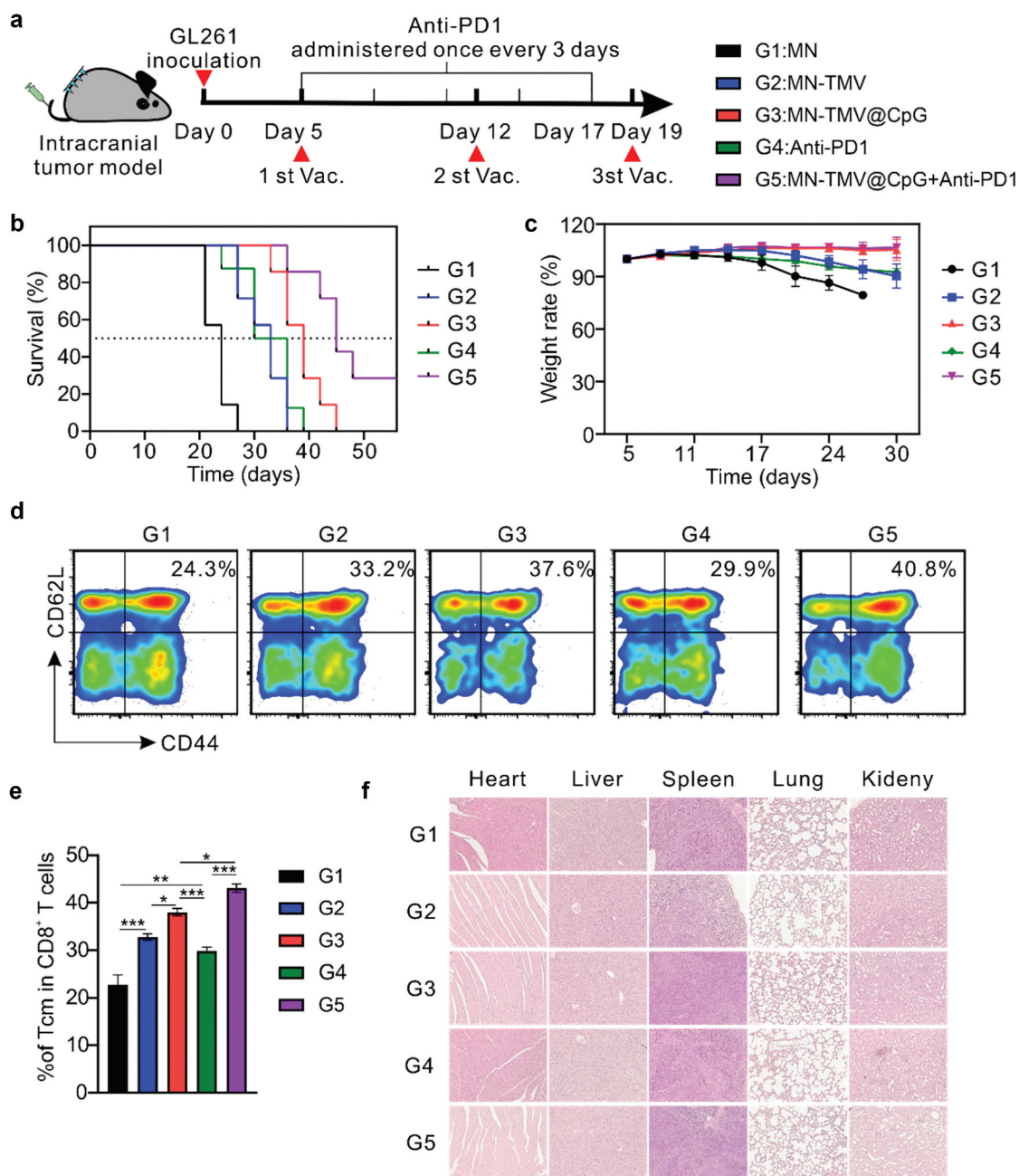


Figure 5. Microneedle vaccine combined with anti-PD1 improved the anti-tumor effect in intracranial tumor model. (a) The protocol of vaccination with MN (G1), MN-TMV (G2), MN-TMV@CpG (G3), anti-PD1 mAb (G4) and MN-TMV@CpG+Anti-PD1 (G5) in C57BL/6J mice with GL261 tumor model. (b) Survival curves with different samples ($n = 7$). (c) Change of body weight of mice during treatment. ($n = 7$). Representative dot plots (d) and quantitative analysis (e) of central memory T cells in the spleen of mice with intracranial loaded tumors, analyzed by flow cytometry ($n = 5$). (f) H&E staining of the main organ after treatment with different formulations ($\times 200$).

MN-TMV@CpG group, which was attributed to its suppression of PD1 expression, resulting in stronger levels of cellular immunity. Finally, we evaluated the safety of the microneedle vaccine. HE staining results for major organs of mice in each group showed that the microneedle vaccine did not form significant damage to the organs of mice (Figure 5(f)). Therefore, we concluded that the biogenic microneedle vaccine not only showed good tumor suppression effect, but also was a relatively safe treatment.

4. Conclusion

Due to the limitations of drugs and immune pathways in the central nervous system, the treatment of gliomas faces great challenges. We have developed a bio-derived tumor vaccine for the treatment of gliomas. Vaccination is carried out through a microneedle delivery method with advantages such as non-invasiveness and convenience. On the one hand, nanovaccines loaded with GelMA hydrogel microneedles can form an antigen reservoir in the skin and play a continuous stimulating role on the body; on the

other hand, microneedles can deliver nanovaccines to the skin and induce a strong cellular immune response using skin-resident antigen-presenting cells.

The results showed that TMV@CpG inherited all the antigenic proteins of tumor cells and could significantly enhance the activation level of BMDCs in vitro (Figures 1(b) and 2(d)). At the same time, the prepared microneedle vaccine had good batch reproducibility and could deliver the vaccine to 140 μm intradermally (Figure 3(b)). In the subcutaneous tumor model, MN-TMV@CpG increased the proportion of cytotoxic T cells in TME, reduced the infiltration of MDSCs, reversed the tumor immunosuppressive microenvironment, and inhibited tumor growth (Figure 4). At the same time, the survival time of mice treated with MN-TMV@CpG and anti-PD1 mAb was significantly enhanced, and strong immune memory was formed, which was conducive to inhibiting the recurrence of glioma (Figure 5).

In addition, the complexity of the nervous system makes it impossible to discern whether the combination of MN-TMV@CpG and anti-PD1 mAb will have adverse effects on the body. With further optimization, we believe that this microneedle-administered biogenic vaccine will provide a new way of thinking for immunotherapy of gliomas.

Disclosure statement

No potential conflict of interest was reported by the author(s).

Funding

This study was supported by the National Natural Science Foundation Project [Grant number: 82271298, CD; 82271297, XL; 82001300, WL].

Data availability statement

Data will be made available on request.

References

- [1] Gargini R, Segura-Collar B, Sánchez-Gómez P. Cellular plasticity and tumor microenvironment in gliomas: the struggle to hit a moving target. *Cancers (Basel)*. 2020;12(6):1622. doi: 10.3390/cancers12061622
- [2] Komori T. Grading of adult diffuse gliomas according to the 2021 WHO classification of tumors of the central nervous system. *Lab Invest*. 2022;102(2):126–133. doi: 10.1038/s41374-021-00667-6
- [3] Lim M, Xia YX, Bettegowda C, et al. Current state of immunotherapy for glioblastoma. *Nat Rev Clin Oncol*. 2018;15(7):422–442. doi: 10.1038/s41571-018-0003-5
- [4] Wu W, Klockow JL, Zhang M, et al. Glioblastoma multiforme (GBM): an overview of current therapies and mechanisms of resistance. *Pharmacol Res*. 2021;171:105780. doi: 10.1016/j.phrs.2021.105780
- [5] van Tellingen O, Yetkin-Arik B, de Gooijer MC, et al. Overcoming the blood-brain tumor barrier for effective glioblastoma treatment. *Drug Resist Update*. 2015;19:1–12. doi: 10.1016/j.drug.2015.02.002
- [6] Huang S, Bai Y, An Z, et al. Gastrodin synergistically increases migration of interleukin-13 receptor $\alpha 2$ chimeric antigen receptor T cell to the brain against glioblastoma multiforme: a preclinical study. *Phytotherapy Res*. 2023;37(12):5947–5957. doi: 10.1002/ptr.8007
- [7] Choe JH, Watchmaker PB, Simic MS, et al. SynNotchcar T cells overcome challenges of specificity, heterogeneity, and persistence in treating glioblastoma. *Sci Transl Med*. 2021;13(591):eabe7378. doi: 10.1126/scitranslmed.abe7378
- [8] O'Rourke DM, Nasrallah MP, Desai A, et al. A single dose of peripherally infused EGFRvIII-directed CAR T cells mediates antigen loss and induces adaptive resistance in patients with recurrent glioblastoma. *Sci Transl Med*. 2017;9(399):eaaa0984. doi: 10.1126/scitranslmed.aaa0984
- [9] Pérez-Larraya JG, Garcia-Moure M, Labiano S, et al. Oncolytic DNX-2401 virus for pediatric diffuse intrinsic pontine glioma. *New Engl J Med*. 2022;386(26):2471–2481. doi: 10.1056/NEJMoa2202028
- [10] Liu PH, Wang YN, Wang YK, et al. Effects of oncolytic viruses and viral vectors on immunity in glioblastoma. *Gene Ther*. 2022;29(3–4):115–126. doi: 10.1038/s41434-020-00207-9
- [11] Friedman GK, Johnston JM, Bag AK, et al. Oncolytic HSV-1 G207 immunovirotherapy for pediatric high-grade gliomas. *New Engl J Med*. 2021;384(17):1613–1622. doi: 10.1056/NEJMoa2024947
- [12] Cloughesy TF, Mochizuki AY, Orpilla JR, et al. Neoadjuvant anti-PD-1 immunotherapy promotes a survival benefit with intratumoral and systemic immune responses in recurrent glioblastoma. Neoadjuvant anti-PD-1 immunotherapy promotes a survival benefit with intratumoral and systemic immune responses in recurrent glioblastoma. *Nat Med*. 2019;25(3):477–486. doi: 10.1038/s41591-018-0337-7
- [13] Reardon DA, Gokhale PC, Klein SR, et al. Glioblastoma eradication following immune checkpoint blockade in an orthotopic, immunocompetent model. *Cancer Immunol Res*. 2016;4(2):124–135. doi: 10.1158/2326-6066.CIR-15-0151
- [14] Omuro A, Vlahovic G, Lim M, et al. Nivolumab with or without ipilimumab in patients with recurrent glioblastoma: results from exploratory phase I cohorts of CheckMate 143. *Neuro Oncol*. 2018;20(5):674–686. doi: 10.1093/neuonc/nox208
- [15] Ji N, Zhang Y, Liu YP, et al. Heat shock protein peptide complex-96 vaccination for newly diagnosed glioblastoma: a phase I, single-arm trial. *JCI Insight*. 2018;3(10):e99145. doi: 10.1172/jci.insight.99145
- [16] Persico P, Lorenzi E, Losurdo A, et al. Precision oncology in lower-grade gliomas: promises and pitfalls of therapeutic strategies targeting IDH-Mutations. *Cancers (Basel)*. 2022;14(5):1125. doi: 10.3390/cancers14051125
- [17] Rutkowski S, De Vleeschouwer S, Kaempgen E, et al. Surgery and adjuvant dendritic cell-based tumour vaccination for patients with relapsed malignant glioma, a feasibility study. *Brit J Cancer*. 2004;91(9):1656–1662. doi: 10.1038/sj.bjc.6602195

- [18] Yamanaka R, Homma J, Yajima N, et al. Clinical evaluation of dendritic cell vaccination for patients with recurrent glioma: results of a clinical phase I/II trial. *Clin Cancer Res.* 2005;11(11):4160–4167. doi: [10.1158/1078-0432.CCR-05-0120](https://doi.org/10.1158/1078-0432.CCR-05-0120)
- [19] Weller M, Butowski N, Tran DD, et al. Rindopepimut with temozolomide for patients with newly diagnosed, EGFRvIII-expressing glioblastoma (ACT IV): a randomised, double-blind, international phase 3 trial. *Lancet Oncol.* 2017;18(10):1373–1385.
- [20] Liau LM, Ashkan K, Tran DD, et al. First results on survival from a large phase 3 clinical trial of an autologous dendritic cell vaccine in newly diagnosed glioblastoma. *J Transl Med.* 2018;16(1):142. doi: [10.1186/s12967-018-1507-6](https://doi.org/10.1186/s12967-018-1507-6)
- [21] Cui Y, Liu J, Cui L, et al. Tumor-targeting and activatable biomimetic nanococktails synergistically regulate immune responses for spatiotemporal immunotherapy of low immunogenic solid tumors. *Nano Today.* 2024;57:102380. doi: [10.1016/j.nantod.2024.102380](https://doi.org/10.1016/j.nantod.2024.102380)
- [22] Liu J, Cui Y, Cabral H, et al. Glucosylated nanovaccines for dendritic cell-targeted antigen delivery and amplified cancer immunotherapy. *ACS Nano.* 2024;18(37):25826–25840. doi: [10.1021/acsnano.4c09053](https://doi.org/10.1021/acsnano.4c09053)
- [23] Fang RH, Gao WW, Zhang LF. Targeting drugs to tumours using cell membrane-coated nanoparticles. *Nat Rev Clin Oncol.* 2023;20(1):33–48. doi: [10.1038/s41571-022-00699-x](https://doi.org/10.1038/s41571-022-00699-x)
- [24] Xu JB, Cao WQ, Wang PL, et al. Tumor-derived membrane vesicles: a promising tool for personalized immunotherapy. *Pharmaceuticals-Base.* 2022;15(7):876. doi: [10.3390/ph15070876](https://doi.org/10.3390/ph15070876)
- [25] An XY, Zeng Y, Liu C, et al. Cellular-membrane-derived vesicles for cancer immunotherapy. *Pharmaceutics.* 2024;16(1):22. doi: [10.3390/pharmaceutics16010022](https://doi.org/10.3390/pharmaceutics16010022)
- [26] Yang R, Xu J, Xu LG, et al. Cancer cell membrane-coated adjuvant nanoparticles with mannose modification for effective anticancer vaccination. *ACS Nano.* 2018;12(6):5121–5129. doi: [10.1021/acsnano.7b09041](https://doi.org/10.1021/acsnano.7b09041)
- [27] Yang Z, Li L, Wei C, et al. Nanovaccine showing potent immunotherapy to tumor by activating $\Gamma\delta$ T cells. *Adv Funct Mater.* 2023;33(44):2303537. doi: [10.1002/adfm.202303537](https://doi.org/10.1002/adfm.202303537)
- [28] Zou MZ, Li ZH, Bai XF, et al. Hybrid vesicles based on autologous tumor cell membrane and bacterial outer membrane to enhance innate immune response and personalized tumor immunotherapy. *Nano Lett.* 2021;21(20):8609–8618. doi: [10.1021/acs.nanolett.1c02482](https://doi.org/10.1021/acs.nanolett.1c02482)
- [29] AL-Japairai KAS, Mahmood S, Almurisi SH, et al. Current trends in polymer microneedle for transdermal drug delivery. *Int J Pharmaceut.* 2020;587:119673. doi: [10.1016/j.ijpharm.2020.119673](https://doi.org/10.1016/j.ijpharm.2020.119673)
- [30] Pielenhofer J, Sohl J, Windbergs M, et al. Current progress in particle-based systems for transdermal vaccine delivery. *Front Immunol.* 2020;11:266. doi: [10.3389/fimmu.2020.00266](https://doi.org/10.3389/fimmu.2020.00266)
- [31] Kriplani P, Guarve K. Transdermal drug delivery: a step towards treatment of cancer. *Recent Pat Anticancer Drug Discov.* 2022;17(3):253–267. doi: [10.2174/1574892816666211202154000](https://doi.org/10.2174/1574892816666211202154000)
- [32] Sheng T, Luo BW, Zhang WT, et al. Microneedle-mediated vaccination: innovation and translation. *Adv Drug Deliver Rev.* 2021;179:113919. doi: [10.1016/j.addr.2021.113919](https://doi.org/10.1016/j.addr.2021.113919)
- [33] Malek-Khatabi A, Razavi MS, Abdollahi A, et al. Recent progress in PLGA-Based microneedle-mediated transdermal drug and vaccine delivery. *Biomater Sci-UK.* 2023;11(16):5390–5409. doi: [10.1039/D3BM00795B](https://doi.org/10.1039/D3BM00795B)
- [34] Edwards C, Shah SA, Gebhardt T, et al. Exploiting unique features of microneedles to modulate immunity. *Adv Mater.* 2023;35(52):e2302410. doi: [10.1002/adma.202302410](https://doi.org/10.1002/adma.202302410)
- [35] Sadiq BA, Mantel I, Blander JM. A comprehensive experimental guide to studying cross-presentation in dendritic cells in vitro. *Curr Protoc Immunol.* 2022;131(1):e115. doi: [10.1002/cpim.115](https://doi.org/10.1002/cpim.115)